

# Determination of Carrier-Envelope Phase of Relativistic Few-Cycle Laser Pulses by Thomson Backscattering Spectroscopy

M. Wen,<sup>1,2</sup> L.L. Jin,<sup>3</sup> H.Y. Wang,<sup>1</sup> Z. Wang,<sup>1</sup> Y.R. Lu,<sup>1</sup> J.E. Chen,<sup>1</sup> and X.Q. Yan<sup>1,4,\*</sup>

<sup>1</sup>*State Key Laboratory of Nuclear Physics and Technology,  
Peking University, Beijing 100871, China*

<sup>2</sup>*Institute of Photonics & Photon-Technology,  
Northwest University, Xi'an 710069, China*

<sup>3</sup>*Department of Physics, Northwest University, Xi'an 710069, China*

<sup>4</sup>*Key Lab of High Energy Density Physics Simulation,  
CAPT, Peking University, Beijing 100871, China*

(Dated: June 21, 2011)

## Abstract

A novel method is proposed to determine the carrier-envelope phase (CEP) of a relativistic few-cycle laser pulse via the central frequency of the isolated light generated from Thomson backscattering (TBS). We theoretically investigate the generation of a uniform flying mirror when a few-cycle drive pulse with relativistic intensity ( $I > 10^{18} \text{W}/\text{cm}^2$ ) interacts with a target combined with a thin and a thick foil. The central frequency of the isolated TBS light generated from the flying mirror shows a sensitive dependence on the CEP of the drive pulse. The obtained results are verified by one dimensional particle in cell (1D-PIC) simulations.

**PACS numbers:** 52.38.Ph, 41.75.Jv, 52.59.Ye, 42.30.Rx

The developments of laser technology provide the possibility to create both the ultrashort and the ultraintense laser sources. Progress in ultrafast laser technology has made it possible to produce laser pulses with only a few cycles in duration [1], which gives a way to attosecond physics and high-order harmonic generation [2]. Meanwhile, the availability of superintense laser pulses opens a window to the physical phenomena occurring in the relativistic and ultra-relativistic domain [3]. With the broad bandwidth material-Ti:sapphire, even few-cycles pulse with peak intensities exceeding  $1 \text{ TW/cm}^2$  and duration of 10 fs or shorter are produced [4]. The focusing of the few-cycle pulse can reach  $\gg 10^{18} \text{ W/cm}^2$  relativistic intensity on the target [5], which is suitable for laser wakefield acceleration regime to generate monoenergetic electrons [6] as well as for high harmonic generation on plasma surfaces [7] and gas jets. For relativistic few-cycle laser, carrier-envelope phase (CEP) measurements are still envisaged for CEP stabilization that will be necessary to generate single attosecond bursts.

The electric field of a laser pulse can be written as  $E(t) = E_0(t) \cos(\omega_L \tau + \phi)$ , with  $E_0(t)$  being the pulse envelope,  $\omega_L$  being the frequency of the carrier wave, and  $\phi$  being the CEP [8]. The CEP  $\phi$  is defined as the offset between the optical phase and the maximum of the wave envelope of an optical pulse. The CEP may affect many processes involving instantaneous laser-matter interaction. On one hand, for few-cycle pulses, it has been proved that the electric field as a function of time depends on the CEP, although the envelope is the same for all pulses. The CEP effects of ultrashort laser pulses are widely investigated from the non-ionizing optics regime [9] to the ionizing intensity regime [10], even to the relativistic regime [11]. On the other hand, with a method for measuring the CEP of a many-cycle pulse [12], CEP effects by intense multi-cycle pulses are experimentally observed [13].

So far, a method known as stereo above threshold ionization (ATI) has been demonstrated experimentally to determine the CEP of few-cycle pulses with intensities up to  $I = 10^{14} - 10^{15} \text{ W/cm}^2$  [14], at a precision of about  $\pi/300$  [15]. Other methods of measuring the CEP are possible through an attosecond photon probe [16] and detection of THz emission generated in a plasma [17]. However, these methods are not available for laser pulses of intensities above  $I = 10^{16} \text{ W/cm}^2$ , when relativistic effects become increasingly important. Recently, a quantum method is proposed to determine the CEP of ultra-relativistic intensity by detecting the angular emission range via multiphoton Compton scattering [18], which is available when the intensity  $I > 10^{20} \text{ W/cm}^2$ . This Letter reports the CEP of a relativistic intense

( $I > 10^{18} \text{W/cm}^2$ ) few-cycle laser pulse can be determined by detecting the spectroscopy of the isolated Thomson Backscattering (TBS) pulse, which is testified by an analytical model and particle in cell simulations.

The corresponding configuration is sketched in Fig. 1(b). In this scheme, an intense few-cycle pulse irradiates a target combined with an ultra-thin (nm) foil and a thick and dense foil (the separation between these two foils is  $x_r$ ). The electrons of the ultra-thin foil driven by the intense pulse play the role of a flying mirror. The thick foil behind will reflect the drive pulse and let only the flying mirror pass through. The flying mirror flies with a relativistic factor  $\gamma_x = 1/\sqrt{1 - \beta_x^2}$ , with  $\beta_x = v_x/c$  being the velocity of the plane flyer in the normal direction. A counter propagating probe light is then mirrored and frequency upshifted by the relativistic Doppler factor, which is  $(1 + \beta_x)/(1 - \beta_x) \approx 4\gamma_x^2$  for  $\gamma_x \gg 1$  [19, 20]. The spectrum of the TBS light, achievable in experiments [21], can be used to determine the CEP of the drive pulse.

For simple understanding, we start with only the ultra-thin foil irradiated by an intense few-cycle laser pulse [see the left part of Fig. 1(a)]. The electrons gain high  $\gamma$  values and the heavy ions are left behind unmoved [22, 23] when the charge separation field is much smaller than the amplitude of the laser field  $E_{L0}$ . The charge separation field depends on the area charge density  $\sigma_0 = en_0d_0$ , where  $n_0$  and  $d_0$  are the plasma density and the foil thickness, respectively. In our analytical model, all equations are presented in the nature unit. The normalized quantities are obtained from their counterparts in SI units marked with prime, i.e., time and length are normalized according to  $t = \omega_L t'$  and  $l = k_L l'$ , field  $E = eE'/(mc\omega_L)$ , vector potential  $a = eA'/(mc)$ , density  $n = n'/n_c$  and momentum  $p = p'/mc$ , where  $e$  and  $m$  are the charge and the mass of the electron,  $\omega_L$  and  $k_L$  are the laser frequency and the wave number,  $c$  is the speed of light in vacuum and  $n_c = \varepsilon_0 m \omega_L^2 / e^2$  is the electron critical density. We use a linearly polarized ( $E_z = 0$ ) pulse with a sine square envelop as the drive pulse

$$E_y = E_{y0} \sin^2(\pi\tau/T) \cos(\tau + \phi), \quad (1)$$

with the propagating coordinate  $\tau = t - x$  and the peak of envelope  $E_{y0}$ . The dynamics are described by the equations [23, 24]

$$\frac{d\kappa}{d\tau} = \left[ \frac{\sigma_0}{2(1 + p_y^2)} \right], \quad (2)$$

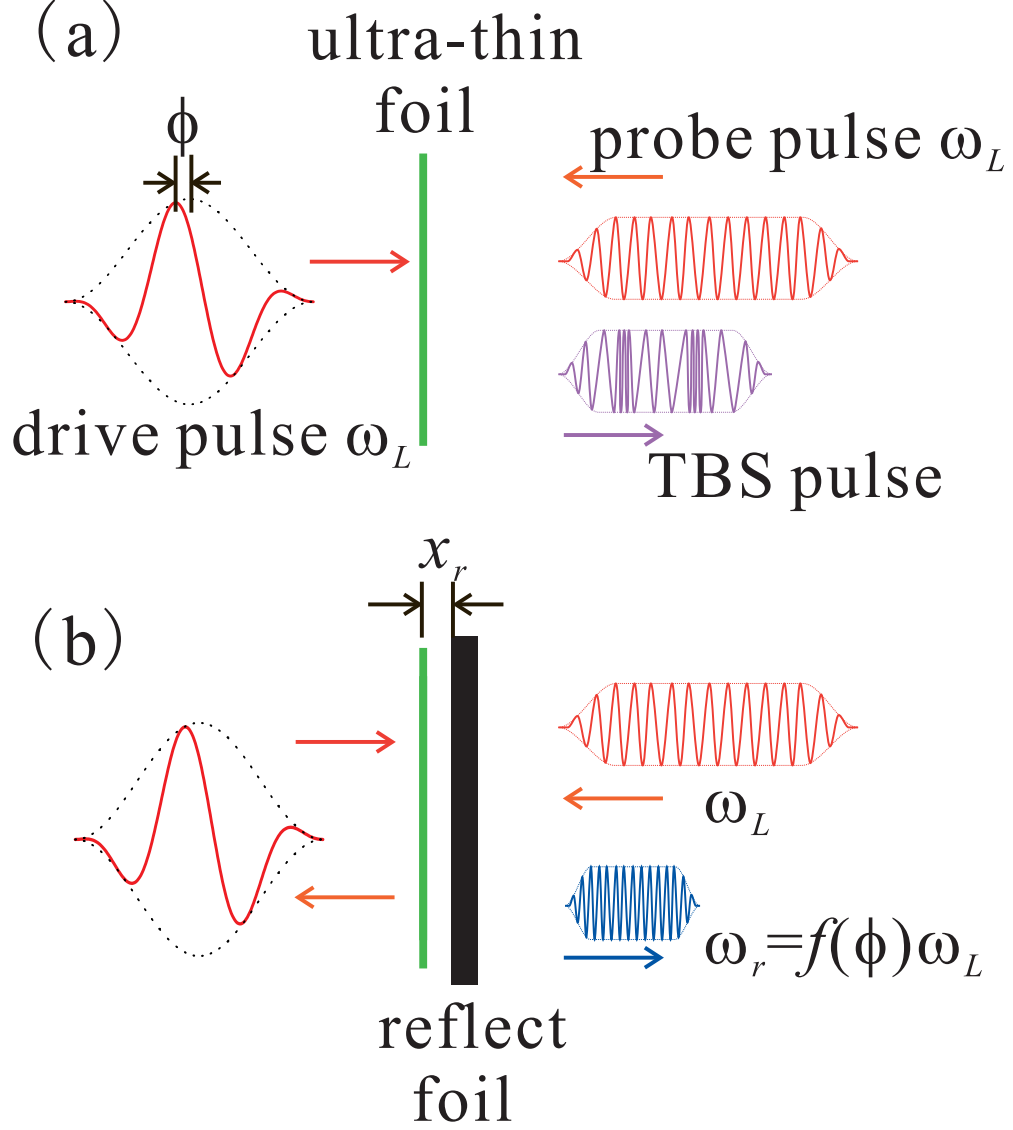


FIG. 1. (Color online) (a) Schematic showing TBS of a weak probe pulse by a flying mirror surfing on a relativistic few-cycle pulse. The scattered pulse is strongly chirped due to the acceleration of the electron layer. (b) Configuration of the CEP measurement with the TBS light. The drive pulse accelerates the flying mirror and is reflected by the reflect foil, without energy consumed. After the relativistic flying mirror flies to the rear side of the reflect foil, a counter propagating probe  $\omega_0$  light is then mirrored and frequency upshifted to  $\omega = f(\phi)\omega_L$ , which highly depends on the CEP of the drive pulse.

$$\frac{dp_y}{d\tau} = -E_y - \left[ \frac{\sigma_0}{2} \frac{p_y}{\kappa} \right]. \quad (3)$$

Here the terms in the square brackets denote the self-fields of the electron layer, and  $E_y$  is the instantaneous laser field when the electron layer surfing in the laser pulse. Analytically,  $\kappa = \gamma - p_x$  and  $p_y$  can be obtained by integrating Eqs. (2) and (3) over the duration  $[0, \tau]$ . With  $\gamma^2 = 1 + p_x^2 + p_y^2$ , one can find that the energy of the flying mirror  $\gamma$  is

$$\gamma = (1 + p_y^2)/2\kappa + \kappa/2. \quad (4)$$

Although the self-radiation and the charge separation field are taken into account in this model, the dominating force is still from the drive pulse. When the charge surface density  $\sigma_0$  is considerably small compared with the laser field  $E_{L0}$ , the analytical model will regress to single electron model  $\kappa \rightarrow 1$  and the energy gain of electron layer is proportional to the square of instantaneous vector potential of the drive pulse

$$\begin{aligned} (\Delta\gamma)^+ &= p_y^2/2 \approx \left[ \int_0^\tau E_y(\tau, \phi) d\tau \right]^2 / 2 \\ &= a_y^2(\tau, \phi)/2 \propto \cos[2\phi + g(\tau)], \end{aligned} \quad (5)$$

where  $g(\tau)$  is a function of  $\tau$ . Equation (5) shows the energy gain of the flying mirror  $(\Delta\gamma)^+$  varies periodically with the CEP of the drive pulse. In other words, a shift of  $\pi$  in the CEP would induce the same results. It shows the energy of the flying mirror is mainly dependent on the temporally varied vector potential  $a_y$ , and carries the detailed information of the drive pulse. Through a proper process to obtain the energy of the flying mirror (TBS shown later), we can extract the CEP of the laser pulse.

We consider a relativistically intense laser field with a peak amplitude of  $E_{y0} = 3.5$ , corresponding to an intensity of  $I = 2.6 \times 10^{19} \text{W/cm}^2$  for  $\lambda_L = 800 \text{nm}$ , with pulse duration  $T = 2\tau_L$ , where  $\lambda_L$  and  $\tau_L$  are laser wavelength and period. The numerical results from our analytical model are plotted in Fig. 2. Figures 2(a) and (b) show that the temporal variation of the electric field and the vector potential depend on the CEP. The energy of the flying mirror during the few-cycle laser field with different CE phases are shown in Figs. 2(c) and (d). Figure 2(c) exhibits how the energy of the flying mirror evolves along the laser propagation  $x$ . It is shown that the peak value of  $\gamma$  depends on the CEP of the relativistically intense laser. The maximal energy of flying mirror can be almost doubled by choosing the CEP properly, e.g.,  $\gamma_{max} = 6.7$  when  $\phi = 0$  (solid curve), while  $\gamma_{max} = 11.8$  when  $\phi = \pi/2$

(dotted curve). If we detect the energy at a fixed position  $x_0$ , it varies periodically with the CEP of the drive laser pulse. A similar trend appears in the dependence of the electron layer energy on time  $t$ , as shown in Fig. 2(d).

Bright VUV- or X-ray source can be obtained by TBS from the relativistic flying mirror. It has been demonstrated that the TBS light from a flying mirror is chirped and has a broad spectrum [20, 25], sketched in Fig. 1(a), which makes it difficult to find a central frequency in the spectrum of the TBS light. However, this can be overcome by setting a thick foil as a reflector behind the ultra-thin foil with a distance  $x_r$  [see Fig. 1(b)], which is a practical way to generate a uniform flying mirror [25, 26]. After the flying mirror emerges from the reflect foil and divorces from the drive laser, its energy  $\gamma$  becomes a constant and depends on the CEP of the pulse [see Fig. 3(a)]. The solid (blue), dashed (green) and dotted (red) curves correspond to  $x_r = \lambda$ ,  $x_r = 1.6\lambda$  and  $x_r = 2.5\lambda$ , respectively. The same with the analytical prediction from Eq. (5),  $\gamma$  is a periodic function of the CEP  $\phi$  with a period of  $\pi$ .

When a probe light irradiates this flying mirror, the frequency of the probe pulse is upshifted by a fixed factor  $\omega_r/\omega_L = 4\gamma_x^2$ , and an isolated pulse with a narrow spectrum is generated. We verify the results by 1D-PIC simulations [27]. The foil parameters in the simulations are the same as those in Ref. [25], i.e., density  $n_0/n_c = 1$  and thickness  $d_0/\lambda_L = 0.001$  for the ultra-thin foil, and  $n_1/n_c = 400$  and  $d_1/\lambda_L = 0.1$  for the reflect foil. The simulation results of the TBS light spectra with different CE phases of the drive pulse are shown in Fig. 3(b) when  $x_r = \lambda$ . We choose  $\phi = 0$ ,  $\phi = \pi/4$ ,  $\phi = \pi/2$  and  $\phi = 3\pi/4$  for examples. As a result of the dependence of the flying mirror energy on the CEP, the central frequency of the spectrum is sensitive to the CEP, e.g., varying from  $\sim 148\omega_L$  at  $\phi = 0$  to  $\sim 357\omega_L$  at  $\phi = \pi/2$ . The central frequency of the TBS light as a periodic function of the CEP predicted by the analytic model is shown in Fig. 3(c).

It should be noticed that the reflected intense light would interact with the flying mirror and cause an energy loss  $(\Delta\gamma)^- \approx 1/2$ , although the interaction is extremely short as compared with the acceleration during the co-moving process with the drive pulse for a long time [20]. After the flying mirror goes through the reflector, its transverse momentum is canceled  $p_y = 0$ , and a very uniform relativistic flying mirror [with the energy  $\gamma_x = \gamma - (\Delta\gamma)^-$ ] is obtained, while the relative energy loss via Coulomb collision is found to be negligible [25]. Taking the CEP of the drive laser into consideration,  $\gamma_x$  depends periodically on the CEP  $\phi$ , illustrated by the right axis in Fig. 3(c). Obeying the relation  $\omega_r/\omega_L = 4\gamma_x^2$ , the central

frequency also exhibits periodicity on the CEP. The analytical predictions agree well with the simulation results.

Due to the period of  $\pi$  we will get two possible phases with one measurement, e.g.  $\omega_r = 200\omega_L$  while  $\phi_1 = 0.27\pi$  and  $\phi_2 = 0.94\pi$  ( $x_r = \lambda$ ). By introducing a second measurement, this restriction can be removed and the CEP can be determined in the range of  $\pi$ . The simulations show when the drive pulse is highly reflected with a limited energy loss [shown in Fig. 3(d)], the drive pulse can be transmitted to another double-foil target again with a different distance  $x_r$ . For example, if the first measurement gives  $\omega_r^{1st} = 200\omega_L$ , for the second measurement with  $x_r = 2.5\lambda$ , the CEP is determined to be  $0.27\pi$  when second measurement gives  $\omega_r^{2nd} = 297\omega_L$ , or  $0.94\pi$  when  $\omega_r^{2nd} = 115\omega_L$ . Moreover, the central frequency is very sensitive to the CEP. For example, around the point  $(0.27\pi|_{\phi}, 200\omega_L|_{\omega_r})$ , a difference of  $1\omega_L$  in the detectable central frequency introduces a phase shift of  $8 \times 10^{-4}\pi$  in the CEP.

In summary, the evolution of a flying mirror driven by a relativistic, few-cycle pulse ( $I = 2.6 \times 10^{19}\text{W/cm}^2$  and  $T \approx 5.3$  fs at  $\lambda = 0.8 \mu\text{m}$ ) from an ultra-thin foil is investigated theoretically. With the help of a reflect foil, a TBS light pulse with narrow spectrum is obtained when a probe light is reflected from the flying mirror. The central frequency of the TBS light is a periodic function of the CEP, with the period of  $\pi$ . The detection of the central frequency of the TBS light makes it possible to determine the CEP of a relativistic few-cycle pulse. We introduce a double-measurement process to determine the CEP in the range of  $\pi$ . In principle, this method is also feasible for a weaker or longer pulses with relativistic intensity ( $I > 10^{18}\text{W/cm}^2$ ), while even thinner foil is needed to generate a uniform flying mirror.

The authors are grateful to Dr. A. Di Piazza for useful discursion. This work was supported by National Nature Science Foundation of China (Grant Nos. 10935002, 11025523, 61008016 and 10905003) and National Basic Research Program of China (Grant No. 2011CB808104). M.Wen and L.L.Jin acknowledges the support from the Scientific Research Program Funded by Shaanxi Provincial Education Department (Program Nos. 11JK0538 and 11JK0529).

---

\* x.yan@pku.edu.cn

- [1] A. Baltuška *et al.*, Nature (London) **421**, 611 (2003); A. Bonvalet *et al.*, Appl. Phys. Lett. **67**, 2907 (1995); G. Krauss *et al.*, Nat. Photon. **4**, 33 (2010); A.L. Cavalieri *et al.*, New J. Phys. **9**, 242 (2007); E. Goulielmakis *et al.*, Science **320**, 1614 (2008).
- [2] F. Krausz and M. Ivanov, Rev. Mod. Phys. **81**, 163 (2009).
- [3] G. Mourou *et al.*, Rev. Mod. Phys. **78**, 309 (2006); V. Yanovsky *et al.*, Opt. Express **16** 2109 (2008); Y. I. Salamin *et al.*, Phys. Rep. **427** 41 (2006).
- [4] A. Stingl *et al.*, Opt. Lett. **20**, 602 (1995); D. H. Sutter *et al.*, Appl. Phys. B **70**, S5 (2000); R. Ell *et al.*, Opt. Lett. **26**, 373 (2001); D. Herrmann *et al.*, Opt. Lett. **34**, 2459 (2009).
- [5] F. S. Tsung *et al.*, Proc. Natl. Acad. Sci. U.S.A. **99**, 29 (2002); L. L. Ji *et al.*, Phys. Rev. Lett. **103**, 215005 (2009).
- [6] K. Schmid *et al.*, Phys. Rev. Lett. **102**, 124801 (2009).
- [7] P. Heissler *et al.*, Appl. Phys. B **101**, 511 (2010); C. D. Tsakiris *et al.*, New J. Phys. **8**, 19 (2006).
- [8] P. Dietrich, F. Krausz, and P. B. Corkum, Opt. Lett. **25**, 16-18 (2000).
- [9] M. Mehendale *et al.*, Opt. Lett. **25**, 1672 (2000); U. Morgner *et al.*, Phys. Rev. Lett. **86**, 5462 (2001); Y. Wu and X. X. Yang, Phys. Rev. A **76**, 013832 (2007); X. T. Xie and M. A. Macovei, Phys. Rev. Lett. **104**, 073902 (2010); K. Xia *et al.*, Phys. Lett. A **361**, 173 (2007).
- [10] G. G. Paulus *et al.*, Nature (London) **414**, 182 (2001); F. Krausz *et al.*, Opt. Photonics News **9**, 46 (1998); A. de Bohan *et al.*, Phys. Rev. Lett. **81**, 1837 (1998); G. Tempea *et al.*, J. Opt. Soc. Am. B **16**, 669 (1999); T. Brabec and F. Krausz, Rev. Mod. Phys. **72**, 545 (2000); C. P. J. Martiny and L. B. Madsen, Phys. Rev. Lett. **97**, 093001 (2006); P. Lan *et al.*, J. Phys B **40**, 403 (2007).
- [11] E. N. Nerush and I. Yu. Kostyukov, Phys. Rev. Lett. **103**, 035001 (2009); S. Varró, Laser Phys. Lett. **3**, 218 (2007).
- [12] P. Tzallas *et al.*, Phys. Rev. A **82**, 061401 (2010); P. Tzallas *et al.*, Nat. Phys. **3**, 846 (2007).
- [13] P. K. Jha *et al.*, Phys. Rev. A **83**, 033404 (2011).
- [14] G.G. Paulus *et al.*, Phys. Rev. Lett. **91**, 253004 (2003).
- [15] T. Wittmann *et al.*, Nature Phys. **5**, 357 (2009).
- [16] E. Goulielmakis *et al.*, Science **305**, 1267 (2004).
- [17] M. Kreß *et al.*, Nature Phys. **2**, 327 (2006).
- [18] F. Mackenroth *et al.*, Phys. Rev. Lett. **105**, 063903 (2010); F. Mackenroth and A. Di Piazza,



- Phys. Rev. A **83**, 032106 (2011).
- [19] A. Einstein, Ann. Phys. (Leipzig) **322**, 891 (1905).
  - [20] J. Meyer-ter-Vehn and H. C. Wu, Eur. Phys. J. D **55** 433(2009); H. C. Wu and J. Meyer-ter-Vehn, Eur. Phys. J. D **55**, 443(2009).
  - [21] Z. Chang *et al.*, Phys. Rev. Lett. **79**, 2967 (1997).
  - [22] V. V. Kulagin *et al.*, Phys. Rev. Lett. **99**, 124801 (2007).
  - [23] M. Wen *et al.*, Eur.Phys. J. D **55**, 451 (2009).
  - [24] H. K. Avetissian, *Relativistic Nonlinear Electrodynamics* (Springer, New York, 2006).
  - [25] H. -C. Wu *et al.*, Phys. Rev. Lett. **104**, 234801 (2010).
  - [26] F. Wang *et al.*, Phys. Plasmas **14**, 083102 (2007).
  - [27] Z. -M. Sheng *et al.*, Phys. Rev. Lett.**85**, 5340 (2000);X.Q. Yan *et al.*, Phys. Rev. Lett.**100**, 135003 (2008).

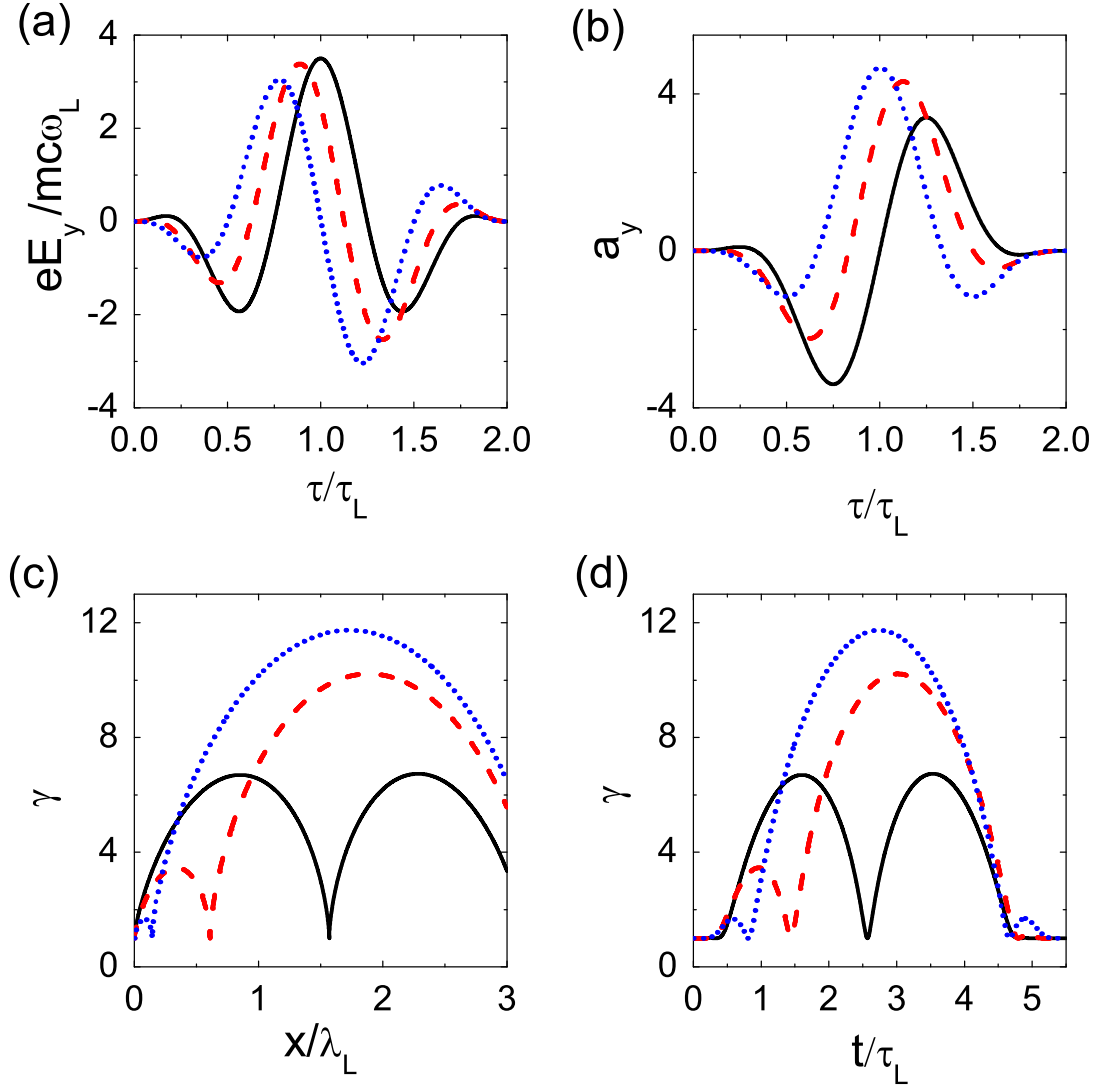


FIG. 2. (Color online) (a) The electric field, (b) vector potential, (c) spatial and (d) temporal evolution of normalized electron layer energy in the few cycle laser field with  $\phi = 0$  [solid (black) curve],  $\pi/4$  [dashed (red) curve] and  $\pi/2$  [dotted (blue) curve] (dotted curve) obtained from analytical model.

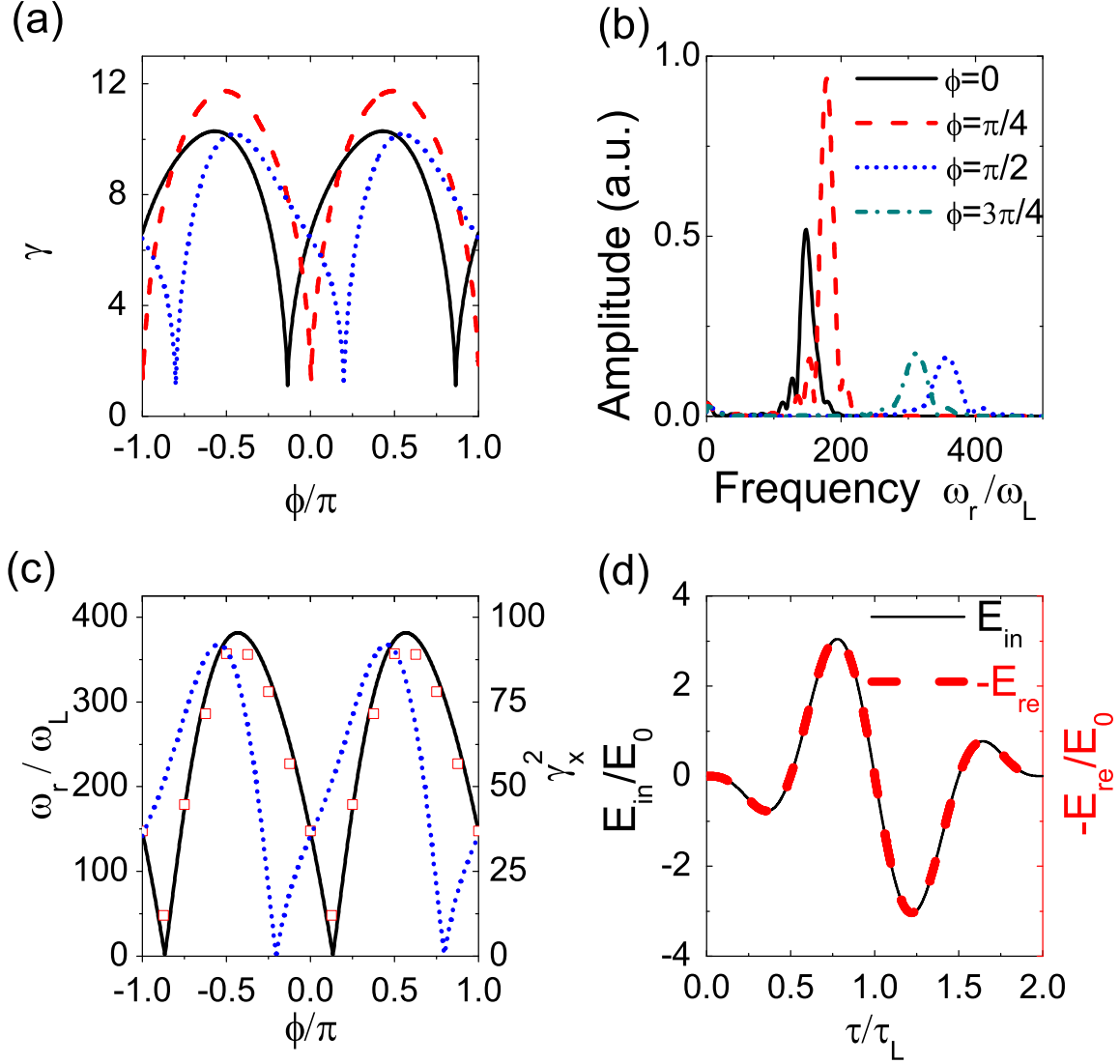


FIG. 3. (Color online) (a) The normalized energy of electron layer  $\gamma$  as functions of the initial CEP of the drive ultrashort pulse, when the electron layer reaches the location of the reflect foil  $x_r$ . The solid (black), dashed (red) and dotted (blue) curves correspond to  $x_r = \lambda$ ,  $1.6\lambda$  and  $2.5\lambda$ , respectively. (b) The spectra of Thomson backscattering light with the CE phases of drive pulses  $\phi = 0, \pi/4, \pi/2$  and  $3\pi/4$  for  $x_r = \lambda$ . (c) When  $x_r = \lambda$  the central frequency of the TBS light as a function of the CEP obtained from the model [(black) solid curve], with the matched simulation results [(red) open cubes]. The (blue) dotted curve represent the dependence of the detected central frequency on the CEP of the drive pulse when  $x_r = 2.5\lambda$ . The electric fields of the incident and reflected drive pulse are compared in (d).